



1 **Improvement of online monitoring technology based on the Berthelot**  
2 **reaction and long path absorption photometer for the measurement of**  
3 **ambient NH<sub>3</sub>: Field applications in low-concentration environments**

4 Shasha Tian<sup>a, b, 1</sup>, Kexin Zu<sup>a, b, 1</sup>, Huabin Dong<sup>a, b, \*</sup>, Limin Zeng<sup>a, b</sup>, Keding Lu<sup>a, b</sup>, Qi Chen<sup>a</sup>

5 <sup>a</sup> State Key Joint Laboratory of Environmental Simulation and Pollution Control, College of  
6 Environmental Sciences and Engineering, Peking University, Beijing, 100871, China.

7 <sup>b</sup> International Joint laboratory for Regional pollution Control (IJRC), Peking University, Beijing,  
8 China

9 \* Corresponding author: hbdong@pku.edu.cn

10

11 **Abstract.** In the last few decades, various techniques, including spectroscopic, wet chemical and  
12 mass spectrometric methods, had been developed and applied for the detection of gaseous ammonia  
13 (NH<sub>3</sub>). We developed an online NH<sub>3</sub> monitoring system (SAC-LOPAP) based on Berthelot reactions and  
14 a long path absorption photometer (LOPAP), which could run statically for a long time and be applied to  
15 the continuous online measurement of low concentrations of ambient air by optimizing the reaction  
16 conditions, adding a constant temperature module and liquid flow controller. The detection limit reached  
17 with this instrument was 40.5 ppt under stable conditions. In addition, the range of NH<sub>3</sub> measurement  
18 varied from background contamination (<40.5 ppt) to approximately 100 ppb in the current condition (a  
19 stripping liquid flow rate of 0.49 ml min<sup>-1</sup> and a gas sample flow rate of 0.70 L min<sup>-1</sup>). An inter-  
20 comparison of our system with another established system in a field campaign in Beijing was presented,  
21 and the results showed that the two instruments had good correlation, indicating that the SAC-LOPAP  
22 involved in this study could be used for the accurate measurement of NH<sub>3</sub>.

23

24

25

26

27

28

29

30



## 31 **1. Introduction**

32 Gaseous ammonia ( $\text{NH}_3$ ) widely exists in the atmosphere and plays an important role in many  
33 atmospheric chemical reactions (Swati and Hait, 2018; Klimczyk et al., 2021; Wang et al., 2018).  
34 As the most abundant alkaline gas in the atmosphere,  $\text{NH}_3$  easily forms ammonium ions ( $\text{NH}_4^+$ )  
35 with water and reacts with acid precursors such as  $\text{SO}_2$  and  $\text{NO}_x$  ( $\text{NO}+\text{NO}_2$ ) to generate secondary  
36 aerosols, which have a significant impact on the generation of particulate matter (Baek and Aneja,  
37 2004; Behera et al., 2013). Kirkby, j. et al. found that trace amounts of  $\text{NH}_3$  (less than 100 ppt) could  
38 increase the nucleation rate of sulfate radicals by 2-10 times in a CLOUD experiment on the  
39 nucleation of new particles. B. Bessagnet et al. found that the estimation of ammonium particle  
40 formation was insufficient, arguing that the role of ammonium in PM was more significant than  
41 initially thought (Bessagnet et al., 2014). In recent decades, the emissions of  $\text{SO}_2$  and  $\text{NO}_x$  have  
42 been controlled to some extent, but the emission reduction of  $\text{NH}_3$  is less than that of  $\text{SO}_2$  and  $\text{NO}_x$   
43 (Scab et al., 2020). Therefore, accurate measurement of  $\text{NH}_3$  is essential for public health and to  
44 further reduce secondary aerosol generation.

45 There are several difficulties in detecting  $\text{NH}_3$  in the atmosphere due to its strong adsorption  
46 and hygroscopicity. The adsorption and hygroscopic properties of  $\text{NH}_3$  are caused by the formation  
47 of a strong hydrogen bond between water and  $\text{NH}_3$  (Hüglin, 2004). Due to the character of  $\text{NH}_3$ , it  
48 can readily be adsorbed on the surface of the sampling tube, resulting in low measurements and  
49 slow response. In particular,  $\text{NH}_3$  is likely to be adsorbed on the metal surface of optical systems in  
50 the spectrometric monitoring instrument, resulting in increased background (Whitehead et al., 2008;  
51 Yokelson and R., 2003). In addition, the temperature difference between the indoor and outdoor  
52 environments and the humidity difference between the inside and outside of the instrument will  
53 reduce the accuracy of measurement and calibration.

54 In recent years, researchers have developed techniques and methods for detecting  $\text{NH}_3$  in the  
55 atmosphere, which include spectroscopic, wet chemical and mass spectrometric methods (Von et al.,  
56 2009). Spectroscopy methods, such as Cavity Enhanced Absorption Spectroscopy (CEAS) (Gong  
57 et al., 2017; Berden et al., 2000) and Cavity Ring-Down Spectroscopy (CRDS) (Qu et al., 2012;  
58 Martin et al., 2016), can greatly improve spectral absorption's effective optical path length by using  
59 the optical cavity structure. However,  $\text{NH}_3$  has a high viscosity and easily adheres to the metal



60 surface of optical systems in spectrometric monitoring instruments, thus affecting the background,  
61 detection efficiency and detection response time of the instrument (Whitehead et al., 2008; Yokelson  
62 and R., 2003). Utilizing a quantum cascade laser (QCL) or a DFB laser in a near-infrared band as  
63 the light source can achieve high detection accuracy and a low detection limit (Gadedjisso-Tossou  
64 et al., 2020), realizing the measurement of low concentrations of  $\text{NH}_3$  in ambient air. The chemical  
65 ionization mass spectrometer (CIMS) technique is based on an ion-molecule reaction to selectively  
66 ionize and detect trace  $\text{NH}_3$  species in the atmosphere, which features a fast response and in situ  
67 measurement (Benson et al., 2010). The sensor measurement method relies on the response of  
68 special materials to  $\text{NH}_3$ . It has the advantages of small volume and wide measurement range, but  
69 its detection limit is very high (Ajay and Beniwal., 2019). Wet chemistry methods usually require a  
70 combination of a wet chemistry collection system and a wet chemistry analyzer, such as a dull-  
71 polished wet tubing denuder (WAD), which can separate gaseous  $\text{NH}_3$  and aerosol particles.  $\text{NH}_3$  is  
72 absorbed and ionized to  $\text{NH}_4^+$  to be analyzed by ion chromatography (Dong et al., 2012). A field  
73 inter-comparison of  $\text{NH}_3$  measurement techniques (Von et al., 2009) found that wet chemistry  
74 instruments showed better long-term stability and agreement than other analyzers, which was due  
75 to the wet chemical trapping method and standard calibration solutions, humidity did not affect the  
76 measurement, and the standard solution was more stable than standard gases. However, they failed  
77 to capture the peak because of lower time resolution. Mass-spectrography analyzers provide highly  
78 sensitive techniques but may be less specific and can be affected by competing ion chemistries.  
79 Furthermore, the Berthelot reaction and absorption spectrophotometry collect  $\text{NH}_3$  (and ammonium)  
80 by aqueous scrubbing in glass frit impactors (Bianchi et al., 2012; Bae et al., 2007), which is a new  
81 wet chemistry method for the determination of  $\text{NH}_3$  that has also been reported by scholars (Bae et  
82 al., 2007).

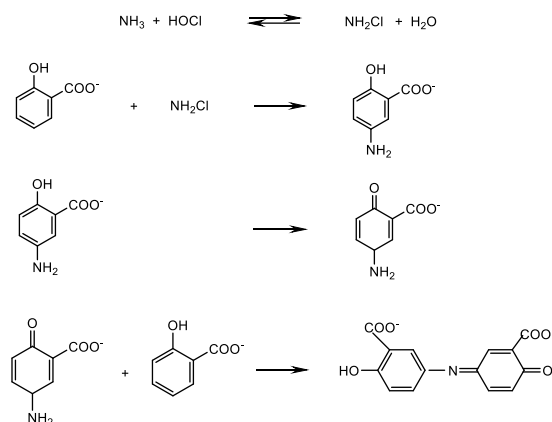
83 In this study, we provide an online  $\text{NH}_3$  monitoring system based on wet chemistry stripping  
84 of atmospheric  $\text{NH}_3$ , followed by the formation of a highly light-absorbing indophenol after a  
85 salicylic acid chromogenic reaction and quantification of the reaction product by a home-made long-  
86 path absorption photometer (LOPAP). We call this monitoring system the salicylic acid  
87 chromogenic and long path absorption photometer (SAC-LOPAP). The objective of this study is to  
88 optimize the key parameters based on the Berthelot reaction and absorption spectrophotometry,



89 establish a method suitable for the instrument can run statically for a long time and can be used for  
90 the continuous online measurement of low concentrations ammonia of ambient air.

## 91 2. Methods

92 Our instrument is designed to measure  $\text{NH}_3$  in a low-concentration environment with the good  
93 stability, low detection limit and small size. There is a brief introduction to the principle of the  
94 instrument. The measurement of  $\text{NH}_3$  in the SAC-LOPAP instrument is achieved by the Berthelot  
95 reaction method. Samples containing dissolved ammonia and ammonium react with a phenolic  
96 compound and a chlorine-donating reagent to form indophenol blue during the reaction, with the  
97 strongest absorption at a wavelength of 665 nm. This reaction is more sensitive than other  
98 chromogenic reactions, such as reactions based on Nessler's reagent (Krom and Michael, 1980;  
99 Searle and Phillip, 1984). Fig. 1 shows the reaction mechanism of the chromogenic reactions.  
100 Furthermore, to measure the absorbance of the sample, we used a long path absorption photometer  
101 (LOPAP) based on liquid-waveguide capillary cell (LWCC) technology to obtain a better detection  
102 limit, continuity and stability (Heland et al., 2001).



103

104

Fig. 1. The reaction mechanism of salicylic acid chromogenic reactions

105 As shown in Fig. 2, we designed our system to consist of four modules: the sampling module,  
106 the reacting module, the detecting module, and the control module. The sampling module contains  
107 a stripping coil (a glass coil in which the air contacts the stripping solution), an air pump, a gas  
108 flowmeter and circulating cooling water. The air is pumped into the stripping coil under the action  
109 of a vacuum diaphragm air pump (Nidec, Japan) and flow meter (Horiba, China) (Chen et al., 2004).

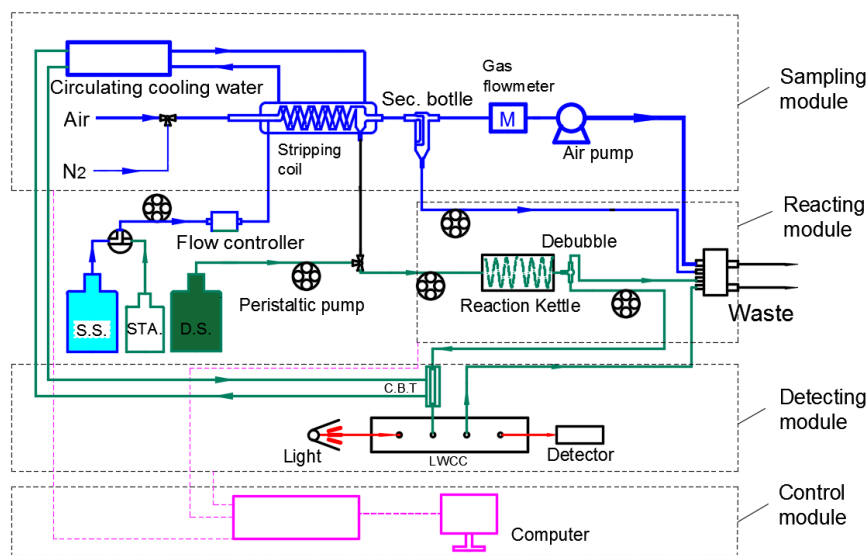


110 At the same time, the stripping solution, regulated by the liquid flow control system, is injected into  
111 the stripping coil to capture  $\text{NH}_3$  components in the air and form a mixture of ammonium-salicylic  
112 acid. To achieve higher absorption efficiency, circulating cooling water with a temperature of 10-15  
113 °C is provided outside the stripping coil. The center part of the reacting module is a reaction kettle  
114 and a debubble. The liquid sample is mixed with an alkaline derivatization solution, and  
115 chromogenic reaction occurs in the heated reaction kettle, which is made of a 90 cm length of Teflon  
116 tubes coiled on a heat-conducting metal cylinder, and the built-in heating rod and temperature sensor  
117 control the temperature of the reactor at 40-75 °C to accelerate the derivatization reaction. After the  
118 chromogenic reaction, the sample is sent to the detecting module, which comprises a liquid  
119 waveguide capillary cell (LWCC, World Precision Instruments, USA), an LED light source, and a  
120 photoelectric detector. The sample solution to be tested is filtered by a 1.0  $\mu\text{m}$  filter before passing  
121 through LWCC to avoid contamination by precipitates in the solution. All instrument functions are  
122 controlled by the control module, including an integrated circuit and a touch panel. The optical path  
123 length of LWCC is 100 cm. The  $\text{NH}_4^+$  standard solution was produced by the National Institute of  
124 Metrology, China.

125 Eq. (1) can help invert the concentration of  $\text{NH}_4^+$  solution  $C_{\text{NH}_4^+}$  to the  $\text{NH}_3$  concentration in  
126 the gas production sample  $C_{\text{NH}_3}$ .

$$127 \quad C_{\text{NH}_3} = \frac{C_{\text{NH}_4^+} F_l R T}{M_{\text{NH}_3} F_g P \gamma} \quad (1)$$

128 Where  $C_{\text{NH}_3}$  denotes the content of  $\text{NH}_3$  in the air sample,  $P$  denotes atmospheric pressure (101.3  
129 kPa),  $M_{\text{NH}_3}$  denotes the molar mass of  $\text{NH}_3$  (g/mol),  $R=8.314 \text{ Pa}\cdot\text{m}^3\cdot\text{mol}^{-1}\cdot\text{K}^{-1}$ .  $T$  denotes the  
130 temperature in the stripping solution (the temperature of the cycling water, the unit is K),  $F_l$  denotes  
131 the flow rate of stripping solution,  $F_g$  denotes the flow rate of sampling gas,  $\gamma$  denotes the capture  
132 efficiency of air  $\text{NH}_3$  in the stripping solution (a constant determined by laboratory).



133

134

Fig. 2. Schematic diagram of SAC-LOPAP

### 135 3 Characterization and optimization

136 We acknowledge that Berthelot reactions must be carried out under catalytic and alkaline conditions.  
137  $[\text{Fe}(\text{CN})_5\text{NO}]^{2-}$  is recognized as a high-efficiency catalytic to increase the sensitivity of the Berthelot  
138 reactions (Krom and Michael, 1980; Searle and Phillip, 1984). However, precipitates containing  
139  $\text{Fe}(\text{OH})_3$  form during the reaction process, which comes from the reaction of  $[\text{Fe}(\text{CN})_5\text{NO}]^{2-}$  with  
140  $\text{NaOH}$ . These precipitates have little effect on off-line instruments. But for on-line instruments,  
141 precipitates can attach to the wall of the pipeline and LWCC, which leads to pipeline blockage and  
142 baseline drift. Therefore, we need to optimize reaction conditions, add the constant temperature  
143 module and liquid flow controller temperature, and so on to achieve continuous online measurement  
144 of low-concentration ammonia in ambient air.

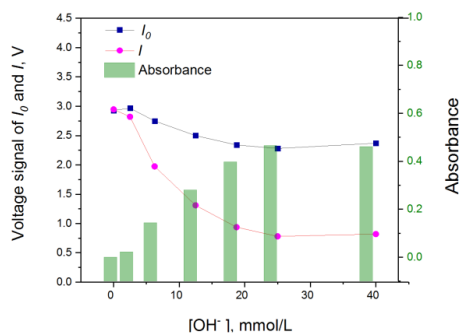
#### 145 3.1 Setting reaction conditions

146 The stripping solution contained  $1 \text{ g L}^{-1} \text{ C}_6\text{H}_4(\text{OH})(\text{COOH})$ ,  $0.1 \text{ g L}^{-1} \text{ s Na}_2[\text{Fe}(\text{CN})_5\text{NO}]^{2-}$ , and  $1 \text{ g}$   
147  $\text{L}^{-1} \text{ NaOH}$ .  $0.5 \text{ ml L}^{-1} \text{ NaClO}$  and  $3 \text{ g L}^{-1} \text{ NaOH}$  were used as derivatization solution based on the  
148 former scholar (Krom and Michael, 1980; Searle and Phillip, 1984), and the state of our experiment  
149 status (Longer optical path and lower sampling volume) in the initial reaction condition. In addition,



150 particulate matter filter was introduced, which could minimize the influence of sediment (Bianchi  
151 et al., 2012), but a large deviation of the baseline would still occur during the long run in our  
152 experiment. According to reaction kinetics, reducing the solution concentration and  $[\text{OH}^-]$  of the  
153 system can greatly reduce the formation of precipitates in the solution. Therefore, we need to find  
154 the optimal reaction conditions to produce the least amount of precipitate. As shown in Figure 3,  
155 higher  $[\text{OH}^-]$  led to a lower voltage signal and higher absorbance, but the effect was no longer  
156 apparent when  $[\text{OH}^-]$  increased to  $18.75 \text{ mmol L}^{-1}$ . We chose an  $18.75 \text{ mmol L}^{-1} \text{ OH}^-$  solution system  
157 with the aim of obtaining a high absorbance of light and a slow speed of precipitate formation, which  
158 meant that  $1.5 \text{ g L}^{-1} \text{ NaOH}$  was added to the derivatization solution. And in this study, the stripping  
159 solution was prepared by dissolving  $0.75 \text{ g L}^{-1} \text{ C}_6\text{H}_4(\text{OH})(\text{COOH})$  (TCI, 99.5%, Japan),  $0.014 \text{ g L}^{-1}$   
160  $\text{Na}_2[\text{Fe}(\text{CN})_5\text{NO}]^{2-}$  (TCI, 99%, Japan), and  $0.2 \text{ g L}^{-1} \text{ NaOH}$ . For the derivatization solution,  $0.188$   
161  $\text{ml L}^{-1} \text{ NaClO}$  (Aladdin, active chlorine 10%, China) and  $1.5 \text{ g L}^{-1} \text{ NaOH}$  were used, which resulted  
162 in the precipitate in the solution being too small to cause pipeline blockage and baseline drift.  
163 Importantly, the concentrations of  $\text{C}_6\text{H}_4(\text{OH})(\text{COOH})$ ,  $\text{Na}_2[\text{Fe}(\text{CN})_5\text{NO}]^{2-}$  and  $\text{NaClO}$  were 96 %,  
164 98 %, and 99 % lower than those in previous research, respectively (Bianchi et al., 2012).

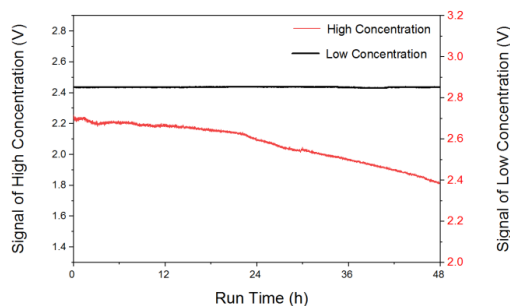
165 In other words, the amount of iron-containing precipitation is very small by reducing the  
166 content of components and alkali of the solution system, and the voltage of the instrument will not  
167 drop significantly due to contamination, which is conducive to better maintenance of the baseline  
168 (Fig. 4).



169

170

Fig. 3. The influence of  $[\text{OH}^-]$  on the voltage signal and absorbance



171

172

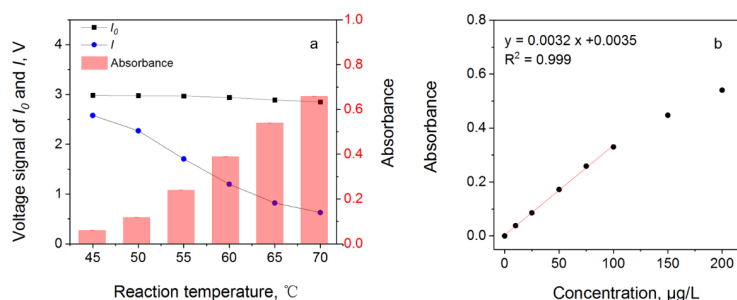
Fig. 4. The blank time series of the  $\text{NH}_3$  detector ran continuously for 72 h.

### 173 3.2 Setup of the temperature

174 However, the reduction of the content of components in the solution will lead to a decrease in  
175 absorbance, so it is necessary to adjust the temperature to speed up the reaction process and achieve  
176 a higher absorbance. As shown in Figure 5a, the voltage signal decreased with increasing  
177 temperature; conversely, the absorbance increased with temperature. However, if the temperature is  
178 too high, there is a danger that the pipeline interface of the instrument will fall off. Considering the  
179 stability and detection range of the instrument, 55 °C was selected as the best reaction operating  
180 temperature of the instrument, at which sufficient absorbance could be achieved to detect low  
181 concentrations of ammonia gas.

182 Furthermore, a high degree of correlation was found between the standard solution and  
183 absorbance with a correlation coefficient of  $R^2 = 0.99$  for the standard solution of 0-100  $\mu\text{g L}^{-1}$  (Fig.  
184 5), indicating that the measurement range was background contamination up to 100  $\mu\text{g L}^{-1}$  for  $\text{NH}_4^+$   
185 solutions. Under the above reaction conditions and temperatures, the detection limit of  $\text{NH}_3$  was  
186 40.5 ppt (gas flow rate of 0.70  $\text{L min}^{-1}$ , liquid flow rate of 0.49  $\text{ml min}^{-1}$ ), the measurement range  
187 was 40.5 ppt up to 100 ppb for  $\text{NH}_3$ , which was well suited for the investigation of the  $\text{NH}_3$  budget  
188 from urban to rural conditions in China. Importantly, the detection limit can be decreased by  
189 improving the gas flow. We can increase our detection range by reducing the temperature and  
190 shortening the length of LWCC. When the temperature drops to 50 °C, the range can be up to 200  
191 ppb. In addition, the minimum reading of the detection signal is 0.1 mV. According to the zero point  
192 data and the calibration, the corresponding concentration to the voltage signal of 0.1 mV is 3.1 ppt,  
193 which far meets our requirements for actual environmental measurement.





194

195

Fig. 5. Influence of reaction temperature on voltage signal and absorbance

### 196 3.3 Stability of liquid flow and temperature

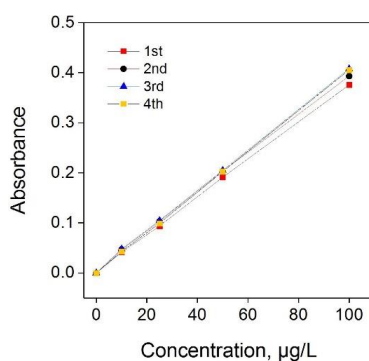
197 The temperature control module and flow control system were designed because of the sensitivity  
198 of chrominance to ambient temperature and residence time. A commercial PID temperature  
199 controller was used to control the temperature of the reaction kettle with the accuracy of  $\pm 0.1$  °C.  
200 The temperature control module was used to control the constant temperature from the reaction  
201 kettle to LWCC at  $55.0 \pm 0.1$  °C. At the same time, the flow control system could control the rotational  
202 speed of the peristaltic. This system used a new type of photoelectric detection to bubbly flow, which  
203 could detect the flow rate and feedback to the peristaltic pump control, which further improved the  
204 stability of the reaction process. In other words, the flow control system could avoid the flow rate  
205 dropping caused by the abrasion of the pump tube and the bump up of the flow rate caused by the  
206 replacement of the pump tube, keeping the stripping solution flow at a constant set point ( $0.49 \text{ ml}$   
207  $\text{min}^{-1}$ ).

208 In addition, we designed a buffer tube with a cooling function to further reduce the effects of  
209 precipitation. After the chromogenic reaction in the reaction kettle at  $55.0$  °C, the mixed solution  
210 entered the cooling buffer tube. Most of the precipitation was generated in the buffer tube and  
211 attached to the tube wall, while some of the precipitation generated in the downstream pipeline was  
212 intercepted by an in-line precipitate filter with a pore size of  $1.0 \mu\text{m}$  before the LWCC.

213 Overall, the above work can make the instrument maintain a relatively stable reaction time and  
214 temperature, which can promote a relatively stable reaction process, resulting in a high  
215 reproducibility to the same concentration of  $\text{NH}_4^+$ . Fig. 6 showed the calibration with the  $\text{NH}_4^+$   
216 concentration gradient of  $0\text{--}100 \mu\text{g L}^{-1}$ , and the relative standard deviations calculated from four



217 consecutive measurements ranged from 0.32 % to 2.65 %. Moreover, the RSD of the blank signal  
218 in continuous operation for one month (blank tests were made every one or two days) was 1.8 %,  
219 showing good stability. After calculating 10-90 % of the full signal after a change in concentration,  
220 the time resolution was approximately 140 s, which was much quicker than the method described  
221 by Bianchi (measured to be 10 min) (Bianchi et al., 2012).



222  
223 Fig. 6. Calibration curves of standard solution with the same concentration gradient 4 times

224 Table 1. Reproducibility test by quickly switching between 50 µg L<sup>-1</sup> NH<sub>4</sub><sup>+</sup> standard and 0 µg L<sup>-1</sup> solution

Number	0 µg L <sup>-1</sup> solution (µg L <sup>-1</sup> )	Response of standard solutions
		(µg L <sup>-1</sup> )
1	-0.014	49.529
2	-0.082	49.615
3	-0.014	50.773
4	0.019	50.599
5	0.053	50.019
6	0.086	50.019
7	-0.048	49.443
AVG	0.000	50.000
STD	0.053	0.484
RSD		0.97%

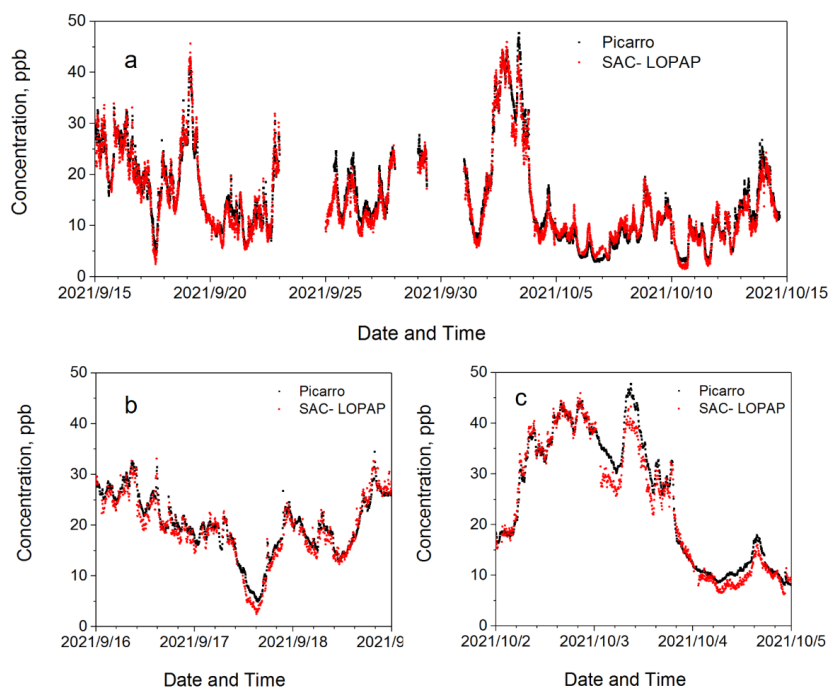
#### 225 4. Field comparison in urban Beijing

226 The field campaign of SAC-LOPAP was conducted at the College of Environment Sciences and  
227 Engineering, Peking University, located within the 4th ring road in northern Beijing (40° N, 116°  
228 E), China. A commercial instrument Picarro G2103 analyzer (Picarro, US) used for atmospheric  
229 NH<sub>3</sub> measurement based on the CRDS method was deployed concurrently with SAC-LOPAP in the  
230 field comparison, which could be used to calibrate and validate other instruments (Twigg et al.,  
231 2022). The inter-comparison experiment took place from 15 September 2021 to 15 October 2021,



232 with the instruments installed in a field container. Two instruments were deployed with a common  
233 inlet height of 2.5 m above the ground. The inlet tube was a 3.8 m long 1/4" Teflon tube covered  
234 with thermo-isolation materials. Additionally, we removed the particles with a Teflon filter at the  
235 front of the sampling inlet and changed the filter every day with the aim of avoiding uncertainties.  
236 Data acquisition times were different for the above instruments during the inter-comparison. The  
237 base reporting periods for Picarro and SAC-LOPAP were 1 s and 30 s. For the purposes of  
238 comparison, data from the two instruments presented in this section were averaged to 5 min. In  
239 addition, zero point was carried out every 7 days, and the standard gas was usually introduced into  
240 the instruments 40 min after zero gas so that they could maintain stability in the measurement  
241 process and ensured quality control.

242 The time series of the concentration of  $\text{NH}_3$  during the inter-comparison period of Picarro and  
243 SAC-LOPAP were presented in Fig. 7a. There were a few data gaps for the above instruments  
244 caused by calibration operations and instrument maintenance. Instruments display similar temporal  
245 features for  $\text{NH}_3$  concentrations over the duration of the study. Fig.7b and Fig.7c showed that the  
246 two instruments had a deviation in response to the peak formed by the rapid rise and fall of  $\text{NH}_3$   
247 concentration, which might be caused by the blank deviation between both instruments. Still, the  
248 response speed was similar, indicated that SAC-LOPAP responded in time to rapid changed in  $\text{NH}_3$   
249 concentration at the five-minute resolution. Furthermore, the  $\text{NH}_3$  concentrations measured by those  
250 instruments were strongly correlated ( $R^2 = 0.967$ ), which significantly indicated that the SAC-  
251 LOPAP developed in this study could measure the  $\text{NH}_3$  concentration accurately. In general, our  
252 instrument run relatively stable with the STD of zero gas during the one month of observations being  
253 within 26 ppt, and both systems agreed for the RSD of the standard gas within 0.76 % (Table 2),  
254 which meant that our instrument could keep steady for a long time and it could be used for the  
255 continuous online measurement of low concentration of ambient air.



256  
 257 Fig. 7. (a) Time series of  $\text{NH}_3$  concentration during the field comparison, and (b), (c) Magnified view of time  
 258 series.

259 Table 2. Reproducibility test by zero gas and standard gas

Test number	Zero gas (ppb)		$\text{NH}_3$ standard (ppb)	
	SAC-LOPAP	Picarro	SAC-LOPAP	Picarro
1	0.014	0.856	40.732	40.291
2	0.074	0.898	40.221	40.072
3	0.069	0.859	40.710	39.995
4	0.031	0.908	40.022	40.011
5	0.062	0.876	40.373	40.076

## 260 5. Conclusions

261 We improved on-line monitoring technology to measure  $\text{NH}_3$  in the atmosphere, which had been  
 262 used for continuous on-line measurement of low concentration ambient air for a long time. Our  
 263 SAC-LOPAP is a combination of the Berthelot reaction and long path absorption photometer for  
 264 gaseous ammonia measurement. It has several notable improvements compared to previous setups,  
 265 as reported by other studies, and one is the optimization of reaction conditions. The low  
 266 concentration but higher flow rate of solutions decreases the precipitate's production, and the



267 cooling buffer tube and the filter trap most of the precipitates. The others are the constant  
268 temperature module and liquid flow controller. The constant temperature module in the system  
269 reduces the influence of ambient temperature on the reaction process and color degree. Similarly,  
270 adding a liquid flow controller is helpful to the stability of the flow rate and further increases the  
271 stability of the reaction process. These improvements reduce the system error and significantly  
272 increase the sustainability of SAC-LOPAP operation. The detection limit reached with this  
273 instrument is 40.5 ppt under stable conditions. The range of  $\text{NH}_3$  measurement vary from  
274 background contamination ( $<40.5$  ppt) to approximately 100 ppb with a stripping liquid flow rate  
275 of  $0.49 \text{ ml min}^{-1}$  and a gas sample flow rate of  $0.70 \text{ L min}^{-1}$  in the current condition. SAC-LOPAP  
276 had a STD of zero point signal within 26 ppt, also agreed for the RSD of the standard gas within  
277 0.76 % within a month, which indicating that the instrument could run statically for a long time and  
278 the repeatability was good. Therefore, we conclude that our update of the ammonia measurement  
279 experimental framework has been successful. However, more research about field measurement and  
280 comparison is needed to verify the equipment's performance in routine observation, and the  
281 influence of particulate ammonium on the results of  $\text{NH}_3$  detection also requires further study.

282

283 **Data availability.** The datasets used in this study are available from the corresponding author upon  
284 request (hbdong@pku.edu.cn).

285

286 **Author contributions.** H.B.D. designed the study. S.S.T., K.X.Z. set up and characterized the  
287 instrument, analyzed the data and wrote the paper with the input of H.B.D. As co-authors, S.S.T and  
288 K.X.Z. contributed equally to this paper. All authors contributed to the field measurements,  
289 discussed and improved the paper.

290

291 **Competing interests.** The authors declare that they have no conflict of interest.

292

293 **Acknowledgments.** This work was supported by special fund of State Key Joint Laboratory of  
294 Environmental Simulation and Pollution Control (Grants No.22Y04ESPCP)

295

296

297

298

299

300

301

302



303 **References.**

- 304 Ajay and Beniwal.: Electrospun SnO<sub>2</sub>/PPy nanocomposite for ultra-low ammonia concentration detection at room  
305 temperature, *Sensors & Actuators B Chemical*, 296, 126660.1-126660.9, <https://doi.org/10.1016/j.snb.2019.126660>,  
306 2019.
- 307 Bae, M. S., Demerjian, K. L., Schwab, J. J., Weimer, S., Hou, J., Zhou, X., Rhoads, K., and Orsini, D.:  
308 Intercomparison of Real Time Ammonium Measurements at Urban and Rural Locations in New York, *Aerosol*  
309 *Science & Technology*, 41, 329-341, <https://doi.org/10.1080/02786820701199710>, 2007.
- 310 Baek, B. H. and Aneja, V. P.: Measurement and analysis of the relationship between ammonia, acid gases, and fine  
311 particles in eastern North Carolina, *Air Repair*, 54, 623-633, <https://doi.org/10.1080/10473289.2004.10470933>, 2004.
- 312 Behera, S. N., Sharma, M., Aneja, V. P., and Balasubramanian, R.: Ammonia in the atmosphere: a review on emission  
313 sources, atmospheric chemistry and deposition on terrestrial bodies, *Environ Sci Pollut Res Int*, 20, 8092-8131,  
314 <https://doi.org/10.1007/s11356-013-2051-9>, 2013.
- 315 Benson, D. R., Markovich, A., Al-Refai, M., and Lee, S. H.: A Chemical Ionization Mass Spectrometer for ambient  
316 measurements of Ammonia, *Atmos. Meas. Tech.*, 3, 1075-1087, <https://doi.org/10.5194/amt-3-1075-2010>, 2010.
- 317 Berden, G., Peeters, R., Meijer, G., and Apituley, A.: Open-path trace gas detection of ammonia based on cavity-  
318 enhanced absorption spectroscopy, *Applied Physics B* 71, 231-216, <https://doi.org/10.1007/s00340000302>, 2000.
- 319 Bessagnet, B., Beauchamp, M., Guerreiro, C., Leeuw, F. D., Tsyro, S., Colette, A., Meleux, F., Roux, L.,  
320 Ruysenaars, P., and Sauter, F.: Can further mitigation of ammonia emissions reduce exceedances of particulate  
321 matter air quality standards?, *Environmental Science & Policy*, 44, 149-163,  
322 <https://doi.org/10.1016/j.envsci.2014.07.011>, 2014.
- 323 Bianchi, F., Dommen, J., Mathot, S., and Baltensperger, U.: On-line determination of ammonia at low pptv mixing  
324 ratios in the CLOUD chamber, *Atmospheric Measurement Techniques*, 5, 1719-1725,  
325 <https://doi.org/10.5194/amt-5-1719-2012>, 2012.
- 326 Chen, X., Oro, Y., Tanaka, K., Takenaka, N., and Bandow, H.: A New Method for Atmospheric Nitrogen Dioxide  
327 Measurements Using the Combination of a Stripping Coil and Fluorescence Detection, *Analytical Sciences the*  
328 *International Journal of the Japan Society for Analytical Chemistry*, 20, 1019,  
329 <https://doi.org/10.2116/analsci.20.1019>, 2004.
- 330 Dong, H. B., Zeng, L. M., Hu, M., Wu, Y. S., Zhang, Y. H., Slanina, J., Zheng, M., Wang, Z. F., and Jansen, R.:  
331 Technical Note: The application of an improved gas and aerosol collector for ambient air pollutants in China,  
332 *ATMOSPHERIC CHEMISTRY AND PHYSICS*, 12, 10519-10533, <https://doi.org/10.5194/acp-12-10519-2012>,  
333 2012.
- 334 Gadedjisso-Tossou, K. S., Stoychev, L. I., Mohou, M. A., Cabrera, H., and Vacchi, A. G.: Cavity Ring-Down  
335 Spectroscopy for Molecular Trace Gas Detection Using A Pulsed DFB QCL Emitting at 6.8  $\mu$ m, *Photonics*, 7, 74,  
336 <https://doi.org/10.3390/photonics7030074>, 2020.
- 337 Gong, D., Liucheng, L. I., Baozeng, L. I., Liping, D., Wang, Y., Yanhua, M. A., Zhang, Z., and Jin, Y.: NH<sub>3</sub>  
338 measurement based on cavity enhanced absorption spectroscopy, *Laser Technology*, 5, 664-668,  
339 <https://doi.org/10.7510/jgjs.issn.1001-3806.2017.05.009>, 2017.
- 340 Heland, J., Kleffmann, J., Kurtenbach, R., and Wiesen, P.: A new instrument to measure gaseous nitrous acid (HONO)  
341 in the atmosphere, *Environmental Science & Technology*, 35, 3207-3212, <https://doi.org/10.1021/es000303t>, 2001.
- 342 Hüglin, E.: Ammonia monitoring at trace level using photoacoustic spectroscopy in industrial and environmental  
343 applications, *Spectrochimica Acta Part A: Molecular and Biomolecular Spectroscopy*, 60, 3259-3268,  
344 <https://doi.org/10.1016/j.saa.2003.11.032>, 2004.
- 345 Klimezyk, M., Siczek, A., and Schimmelpfennig, L.: Improving the efficiency of urea-based fertilization leading to  
346 reduction in ammonia emission, *Science of The Total Environment*, 771, 145483,



- 347 <https://doi.org/10.1016/j.scitotenv.2021.145483>, 2021.
- 348 Krom and Michael, D.: Spectrophotometric determination of ammonia: a study of a modified Berthelot reaction  
349 using salicylate and dichloroisocyanurate, *Analyst*, 105, 305-316, <https://doi.org/10.1039/an9800500305>, 1980.
- 350 Martin, N. A., Ferracci, V., Cassidy, N., and Hoffnagle, J. A.: The application of a cavity ring-down spectrometer to  
351 measurements of ambient ammonia using traceable primary standard gas mixtures, *Applied Physics B*, 122, 219,  
352 <https://doi.org/10.1007/s00340-016-6486-9>, 2016.
- 353 Qu, Z. C., Li, B. C., and Han, Y. L.: Cavity ring-down spectroscopy for trace ammonia detection, *Journal of Infrared  
354 & Millimeter Waves*, 31, 431-436, <https://doi.org/10.3724/SP.J.1010.2012.00431>, 2012.
- 355 Scab, C., Mc, D., Zheng, G. E., Wen, X. F., Xdd, G., and Yu, L.: Enhanced atmospheric ammonia (NH<sub>3</sub>) pollution  
356 in China from 2008 to 2016: Evidence from a combination of observations and emissions - ScienceDirect,  
357 *Environmental Pollution*, 263, <https://doi.org/10.1016/j.envpol.2020.114421>, 2020.
- 358 Searle and Phillip, L.: The berthelot or indophenol reaction and its use in the analytical chemistry of nitrogen. A  
359 review, *Analyst*, 109, 549-540, <https://doi.org/10.1039/an9840900549>, 1984.
- 360 Swati, A. and Hait, S.: Greenhouse Gas Emission During Composting and Vermicomposting of Organic Wastes – A  
361 Review, *CLEAN - Soil Air Water*, 46, 1700042.1-1700042.3, <https://doi.org/10.1002/clean.201700042>, 2018.
- 362 Twigg, M. M., Berkhout, A. J. C., Cowan, N., Crunaire, S., Dammers, E., Ebert, V., Gaudion, V., Haaima, M., Häni,  
363 C., John, L., Jones, M. R., Kamps, B., Kentisbeer, J., Kupper, T., Leeson, S. R., Leuenberger, D., Lüttschwager, N.,  
364 O. B., Makkonen, U., Martin, N. A., Missler, D., Mounsor, D., Neffel, A., Nelson, C., Nemitz, E., Oudwater, R.,  
365 Pascale, C., Petit, J. E., Pogany, A., Redon, N., Sintermann, J., Stephens, A., Sutton, M. A., Tang, Y. S., Zijlman, R.,  
366 Braban, C. F., and Niederhauser, B.: Intercomparison of in situ measurements of ambient NH<sub>3</sub>: instrument  
367 performance and application under field conditions, *Atmos. Meas. Tech.*, 15, 6755-6787,  
368 <https://doi.org/10.5194/amt-15-6755-2022>, 2022.
- 369 Von, B. K., Braban, C. F., Famulari, D., Jones, S. K., Blackall, T., Smith, T., Blom, M., Coe, H., Gallagher, M., and  
370 Ghalaieny, M.: Field inter-comparison of eleven atmospheric ammonia measurement techniques, *Atmospheric  
371 Measurement Techniques*, 3, 91-112, <https://doi.org/10.5194/amt-3-91-2010>, 2009.
- 372 Wang, Ruyu, Ye, Xingnan, Liu, Yuxuan, Li, Haowen, Yang, and Xin: Characteristics of atmospheric ammonia and  
373 its relationship with vehicle emissions in a megacity in China, *Atmospheric Environment*, 182, 97-104,  
374 <https://doi.org/10.1016/j.atmosenv.2018.03.047>, 2018.
- 375 Whitehead, J. D., Twigg, M., Famulari, D., Nemitz, E., Sutton, M. A., Gallagher, M. W., and Fowler, D.: Evaluation  
376 of Laser Absorption Spectroscopy Techniques for Eddy Covariance Flux Measurements of Ammonia, *Environmental  
377 Science & Technology*, 42, 2041-2046, <https://doi.org/10.1021/es071596u>, 2008.
- 378 Yokelson and R., J.: Evaluation of adsorption effects on measurements of ammonia, acetic acid, and methanol,  
379 *Journal of Geophysical Research Atmospheres*, 108, <https://doi.org/10.1029/2003JD003549>, 2003.
- 380